Isobar Production Mechanisms in Proton-Proton Collisions at 5 GeV/c*†

A. P. COLLERAINE‡ AND U. NAUENBERG
Palmer Physical Laboratory, and Princeton-Pennsylvania Accelerator, Princeton University, Princeton, New Jersey

(Received 31 March 1967)

Approximately 7500 four-prong proton-proton collisions at 5 GeV/c have been studied using the BNL 80-in. hydrogen bubble chamber. The three principal reactions studied with their cross sections are:

(a) $p+p \rightarrow p+p+\pi^+ +\pi^-$ 2.96±0.12 mb,
(b) $p+p \rightarrow p+p+\pi^+ +\pi^- +\pi^0$ 1.76±0.07 mb,
(c) $p+p \rightarrow p+n+\pi^+ +\pi^+ +\pi^-$ 2.19±0.09 mb.

In each reaction both single and double N^* production occurs and the decay angular distributions and density matrix elements have been calculated whenever possible. These parameters indicate that pseudoscalar (pion) exchange appears to be dominant at low values of momentum transfer and that at higher momentum transfer absorptive effects become important. We find no evidence for ρ exchange in the reaction $p+p \rightarrow N^{*++}+N^{*0}$. The formation of the η- and ω-meson resonances is observed in reaction (b), but in none of the reactions studied is any significant ρ-meson production found to occur. In reaction (c) we find a deviation from phase space in the region of the 1580-MeV mass bump in the $p\pi^+\pi^+$ ($I=\frac{3}{2}$) system which was observed by Alexander *et al.*, but we ascribe this departure from phase space at our energy as being principally due to N^{*++} and N^{*-} formation in this channel.

I. EXPERIMENTAL PROCEDURE

THE data for this experiment were obtained at the Brookhaven National Laboratory in an exposure of the 80-in. hydrogen bubble chamber to 5-GeV/c protons from the alternating gradient synchrotron. Approximately 10^5 pictures were used and there was an average of 14 beam tracks per picture. The details of the experiment have appeared elsewhere.[1]

A. The Beam

The beam transport system[2] produced a proton beam of nominal momentum 5 GeV/c at the bubble chamber. The actual momentum of the particles entering the chamber was determined by measuring a sample of 400 noninteracting beam tracks and processing these with the THRESH–GRIND[3] geometrical-reconstruction and kinematic-fitting programs using the chamber optical constants and magnetic field as measured at Brookhaven.[4] Each track was measured over a length of about 120 cm, and it was found that the momentum at the $x=0$ plane (first fiducial after the beam entrance to the chamber) was $P=(4.95\pm0.03)$ GeV/c.

B. Scanning Procedure

The film used in looking for four-prong interactions was actually scanned twice, in each case using all three stereoscopic views to avoid missing good events which are obscured by neighboring beam tracks in one view. All events which could be identified in one or more views were recorded and used for the cross-section determination, but not all events found could be measured because of imperfections in the bubble-chamber illumination or because of gross confusion with other tracks (8% of the events were not measured for these reasons). Approximately 10% of the measurable events were seen to have a subsequent interaction of one of the outgoing tracks. If the track connecting the primary vertex with such a secondary interaction had a sagitta greater than 0.25 cm (in space), the secondary interaction was disregarded. However, if this sagitta requirement was not fulfilled, the secondary interaction was recorded with the instruction that it be measured as part of the event. Such a measurement gives additional information on the identity of the connecting track which is useful in cases where the sagitta is so small that the momentum of the connecting track is poorly defined. During the scanning a fiducial region was defined by accepting as events only those interactions in which the primary vertex fell within the limits $0.0 \leq x \leq 126.4$ cm; this is the distance between the two extreme fiducial marks (fiducials 4a and 7a of Ref. 4). No conditions were imposed on the Y or Z values of the coordinates of the primary vertex. The reasons for choosing this fiducial region were twofold: (1) It enabled us to eliminate the tasks of scanning and estimating track ionizations in those regions of the chamber where bubble formation and photography were poor; (2) only events with tracks long enough for

* Work supported by the U. S. Atomic Energy Commission.
† This work made use of computer facilities supported in part by a National Science Foundation Grant No. NSF GP 579.
‡ Submitted in partial fulfillment of the requirements for the degree of Doctor of Philosophy at Princeton University.
[1] A. P. Colleraine, Ph.D. thesis, Princeton University, 1966 (unpublished); Princeton Pennsylvania Accelerator Report No. PPAD-600 F, 1966 (unpublished).
[2] I. Skillicorn and M. S. Webster, Brookhaven National Laboratory Bubble Chamber Report No. BC-H-10 (unpublished).
[3] THRESH: A. M. Cnops, CERN Report No. DD/EXP/63/12, 1963 (unpublished); GRIND: R. Böck, CERN Report No. DD/EXP/62/10, 1962 (unpublished).
[4] E. L. Hart, Brookhaven National Laboratory Bubble Chmaber Report No. BC-04-3-B, 1965 (unpublished).

accurate momentum determination would be accepted for further study. The fiducial region was also used in finding the actual path length of beam track scanned for the purpose of calculating the cross sections. Our overall scanning efficiency for the two scans was 99.1%.

C. Event Measurement and Data Reduction

Each four-prong event found which satisfied the above requirements was measured on a Vanguard measuring machine. In addition to recording each track the operator was asked to estimate the ionization of the track relative to a nearby "minimum ionizing" beam track using the following scale: minimum, grey, dark, and black. Two special codes were set aside for protons stopping in the chamber and for obvious pion tracks (identified by the $\pi \rightarrow \mu \rightarrow e$ decay sequence). This apparently crude scale of ionizations was found to be perfectly acceptable and enabled a unique kinematic fit to be selected for all but about 500 of the events measured; these latter events were reexamined by a scanner using finer gradations of ionization.

The data produced by the measuring machines was punched on to IBM cards in the early phase of the experiment; this procedure was replaced by writing each complete event directly onto magnetic tape after exhaustive checking for operator errors by a PDP-5 computer on line to the measuring machines.[5]

Each event was subsequently processed with the THRESH and GRIND computer programs. The successful kinematic fits produced were checked by a third computer program to see (1) that there were no faults in measurement or spatial reconstruction (determined by flags set by the program THRESH); (2) that the probability of the fit was greater than 1%; and (3) that the calculated ionization for each track was consistent with that assigned by the measurer. (This usually permitted the correct fit to be chosen for those events where two or more fits were kinematically possible.) Events which satisfied all of these criteria were placed in one of the five categories represented by the following reactions:

(i) $p+p \rightarrow p+p+\pi^+ +\pi^-$,
(ii) $p+p \rightarrow p+n+\pi^+ +\pi^+ +\pi^-$,
(iii) $p+p \rightarrow p+p+\pi^+ +\pi^- +\pi^0$,
(iv) $p+p \rightarrow d+\pi^+ +\pi^+ +\pi^-$,
(v) $p+p \rightarrow d+\pi^+ +\pi^+ +\pi^- +\pi^0$.

Events which failed any of the above criteria were treated as follows:

(a) Any event with a measurement or geometry error was returned for remeasurement; some 15% of the events fell into this category. If, after three successive measurements, an event still had an error it was listed as unmeasurable. The 372 such events which remained have been taken into account in the cross-section determination.

(b) Events with no kinematic fit, or with fits with probability less than 1%, were examined to determine if they would be consistent with the hypothesis that two or more neutral particles were produced. Approximately 1700 events fell into this category—they were not remeasured.

(c) Events possessing more than one kinematically possible fit, which corresponded with the observed track ionization within the limits of the scale previously mentioned, were examined by an experienced scanner.

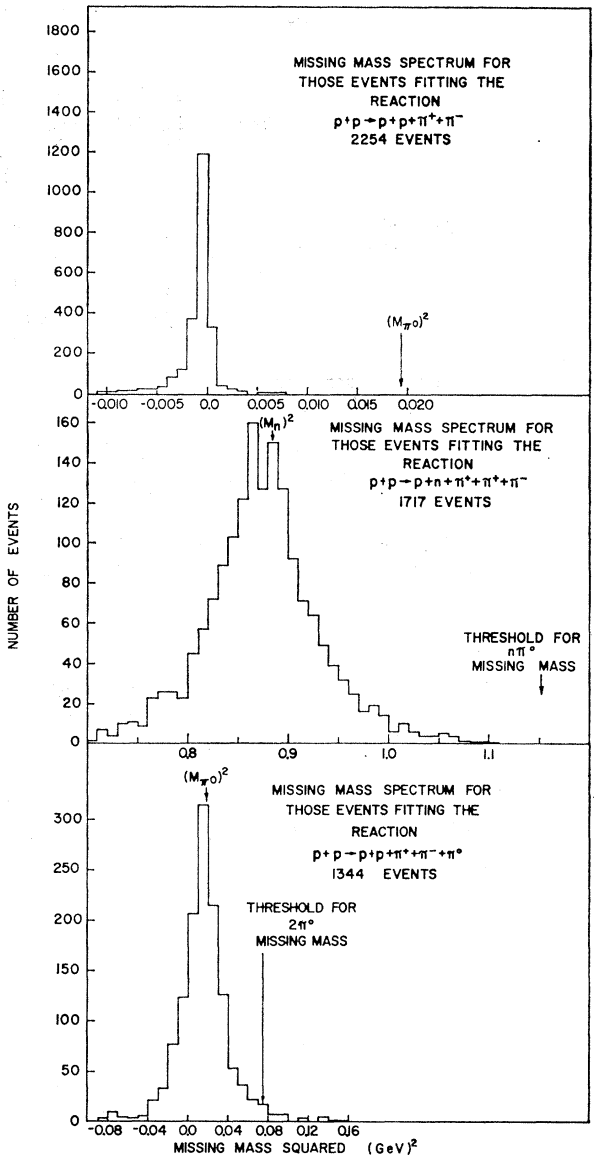

FIG. 1. Missing-mass plots for the final states $pp\pi^+\pi^-$, $pn\pi^+\pi^+\pi^-$, and $pp\pi^+\pi^-\pi^0$.

[5] M. Bazin, J. Benoit, H. Blumenfeld, U. Nauenberg, and R. Zacher, Princeton Pennsylvania Accelerator Report No. PPAD 2137-549, 1965 (unpublished).

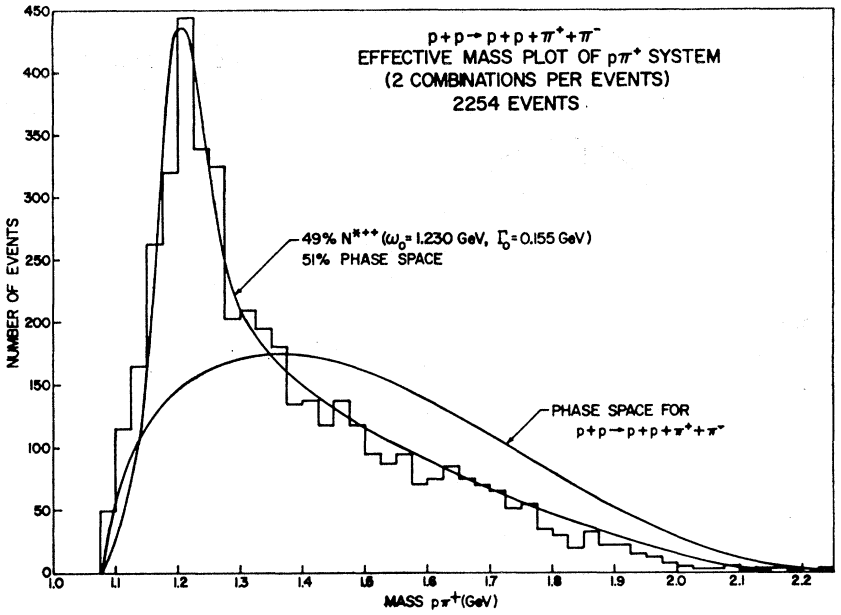

FIG. 2. Effective-mass plot of the $p\pi^+$ system for reaction (i).

The correct fit could almost always be chosen by using finer gradations of ionization than those employed in the computer programs. About 400 events were successfully treated in this way while a further 90 were still ambiguous between reactions (1) and (2), and in this case 45 of the events were added to each of the two classes.

(d) Events with a good probability of fit and no measurement or geometry faults which had predicted track ionization in disagreement with the observed ionizations were first examined to determine whether the measurer had made a mistake in assigning the ionization code. If such a mistake had occurred, it was corrected and the event recycled. If no such mistake was evident, the event was remeasured. About 400 events were treated in this way.

A useful way of displaying the ability of the kinematics program to select events and fit them to a given hypothesis is to plot the missing-mass spectrum for that hypothesis. Figure 1 shows such plots for the reactions (i), (ii), and (iii), The square of the missing mass was calculated using the measured values of momentum and angles for events which satisfied the selection criteria discussed above. The plots for reactions (i) and (ii) indicate that there is no background from events where an additional π^0 is produced. In reaction (iii) the background from double π^0 production is at most 3.5%, and is more probably less than 0.5% if we assume that double π^0 production follows phase space.

D. Cross-Section Determination

To find the total length of beam track scanned, a beam count was made on every 20th frame of the film used. In 825 frames there were 2003 interactions of beam protons and the total length of beam track was $(1.30\pm0.01)\times10^6$ cm. Using these figures and the known value of the proton-proton total cross section, namely $\sigma_T=43.5\pm1.5$ mb,[6] we obtain the hydrogen density as $\rho=(0.061\pm0.002)$ g cm^{-3}, which is in good agreement with the average value 0.062 gcm^{-3} derived from the vapor pressure of the chamber during the exposure. The contamination of the incoming beam was determined by making a scan for energetic δ rays in every 10th frame of the film used. Only one δ ray with kinetic energy greater than 28.5 MeV (the kinematic maximum for proton-electron collision in the present experiment) was found in 2.78×10^6 cm of beam track, and this indicates that the contamination due to particles lighter than protons is only about one in a thousand. Table I shows the values obtained for the cross section of reactions (i) through (v). The errors shown include the errors in the determination of the hydrogen density, the scanning efficiency, and the beam count, in addition to the statistical error in the number of events. The asymmetry of this error in the last reaction reflects

TABLE I. Cross sections.

Reaction	Number of events	Cross section (mb)
$p+p\rightarrow p+p+\pi^++\pi^-$	2680	$2.96+0.12$
$p+p\rightarrow p+p+\pi^++\pi^-+\pi^0$	1592	1.76 ± 0.07
$p+p\rightarrow p+n+\pi^++\pi^++\pi^-$	1985	2.19 ± 0.09
$p+p\rightarrow d+\pi^++\pi^++\pi^-$	21	0.02 ± 0.01
$p+p\rightarrow d+\pi^++\pi^++\pi^-+\pi^0$	73	$0.08_{-0.03}{}^{+0.01}$

[6] T. Fujii, G. B. Chadwick, G. B. Collins, P. J. Duke, N. C. Hein, M. A. R. Kemp, and F. Turkot, Phys. Rev. 128, 1836 (1962); 129, 2835(E) (1963).

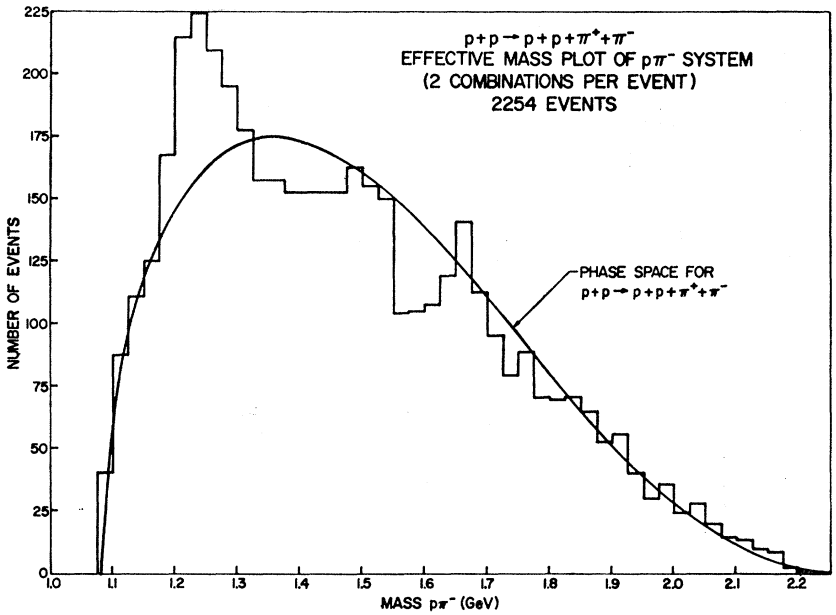

FIG. 3. Effective-mass plot of the $p\pi^-$ system for reaction (i).

the difficulty in distinguishing high-momentum ($\gtrsim$2.5 GeV/c) deuterons from protons.

II. ANALYSIS OF THE DATA

We analyze our data in terms of the one-particle-exchange model which has been rather successful in describing a large body of experimental data in this energy region and, as we shall see, can satisfactorily describe the data of this experiment also. The derivations of the formulas used here have been presented elsewhere.[1]

A. The Reaction $p+p \to p+p+\pi^+ +\pi^-$

The striking feature of this reaction is seen immediately from the combined mass distributions of the $p\pi^+$ and $p\pi^-$ systems shown, respectively, in Figs. 2 and 3. In each graph two combinations of the $p\pi$ mass are shown for each event because of the indistinguishability of the two protons. The departure from phase space is obvious in both cases; strong $N^{*++}{}_{3/2,3/2}(1236$ MeV) formation is observed in the $p\pi^+$ spectrum, while $N^{*0}{}_{3/2,3/2}(1236)$, $N^{*0}{}_{3/2,1/2}(1512)$, and $N^{*0}{}_{5/2,1/2}(1688)$ formation occurs in the $p\pi^-$ spectrum. (The notation used is $N^*{}_{J,I}$, where J is the spin and I the isospin of the isobar.) Such pronounced isobar formation suggests that the double isobar diagram of Fig. 4, in which c and d are resonances, might play a major role in the interaction. Furthermore, Fig. 5 shows that the production angular distribution of the $p\pi^+$ system is peaked at small values of θ^* (the center-of-mass scattering angle) characteristic of a peripheral interaction. The forward-backward symmetry exhibited arises from the indistinguishability of the two protons.

Because of the effects of the N^* propagator the experimental peak of the $N^{*++}(1236)$ is shifted to lower mass values. Jackson[7] has shown that for this resonance the experimental peak should be lower than the theoretical value by approximately 23 MeV. This is seen to be in

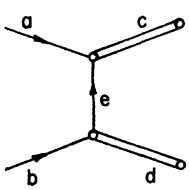

FIG. 4. Lowest-order diagram for double resonance formation.

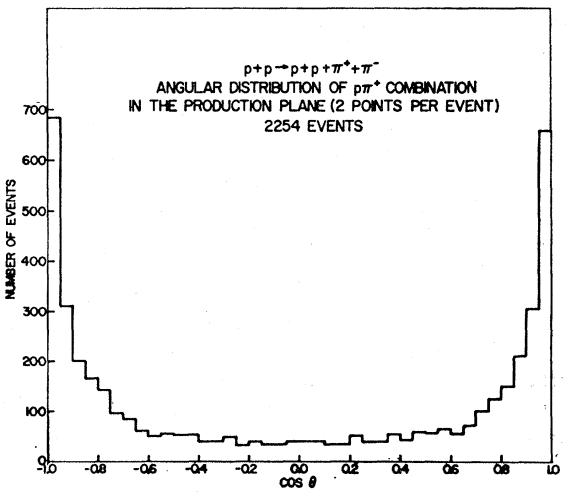

FIG. 5. Angular distribution of the $p\pi^+$ combination in the production center-of-mass system for reaction (i).

[7] J. D. Jackson, Nuovo Cimento 34, 1644 (1965).

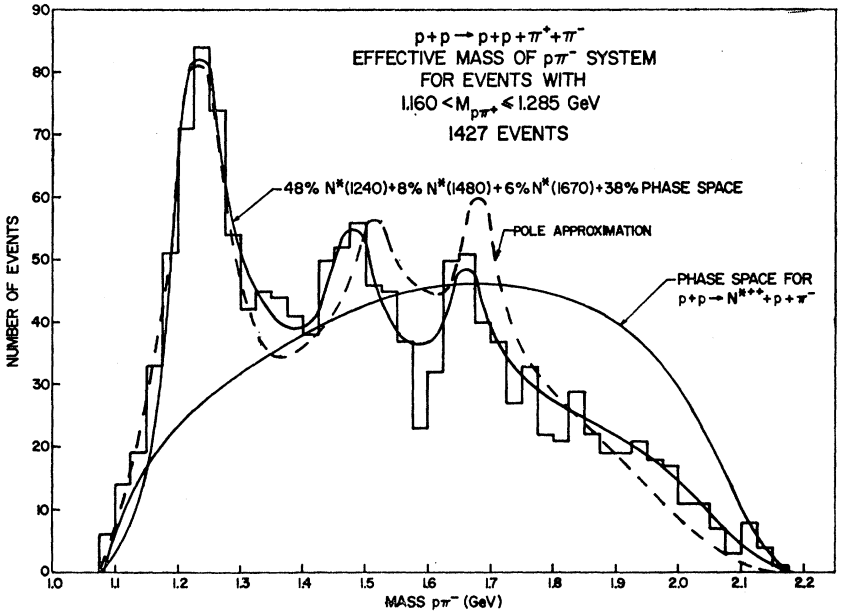

FIG. 6. Effective mass of the $p\pi^-$ system of reaction (i) for those events with an $N^{*++}(1236)$.

reasonable agreement with the data shown in Fig. 2, where the peak occurs at 1.212 GeV. Also shown in Fig. 2 is the minimum χ^2 fit of the data to a resonance and phase space. The cross section for a resonance of intrinsic mass ω_0 and width Γ_0 is represented by

$$d\sigma=\frac{d\sigma_s(\omega)}{\pi}\frac{\omega_0\Gamma(\omega)}{(\omega_0^2-\omega^2)^2+\omega_0^2\Gamma^2(\omega)}d\omega^2, \qquad (1)$$

in which the energy-dependent width $\Gamma(\omega)$ is expressed in terms of Γ_0 by

$$\Gamma(\omega)=\Gamma_0\left(\frac{q}{q_0}\right)^{2l+1}\frac{(\omega+M)^2-m_p^2}{(\omega_0+M)^2-m_p^2}\left(\frac{\omega_0}{\omega}\right)^2, \qquad (2)$$

where q is the momentum of one of the decay products in the rest frame of the N^* calculated for a resonant mass ω, while q_0 is the momentum calculated for the intrinsic resonant mass ω_0, and the relative orbital-angular-momentum state of the pion-nucleon system is l. M and m_p are the masses of the decay baryon and pion, respectively.

If $\phi(\omega)$ represents the phase-space distribution and $R(\omega_0,\Gamma_0)$ represents the resonance term, the data of Fig. 2 may be fitted to the equation

$$\frac{dN(\omega)}{d\omega}=[aR(\omega_0,\Gamma_0)+b]\phi(\omega), \qquad (3)$$

where $N(\omega)$ is the number of events as a function of the mass ω of the $p\pi^+$ system and a and b represent the relative production rates of the resonant and nonresonant terms in the distribution, respectively. The probability of the fit shown in Fig. 2 is less than 1% mainly because the lowest two mass intervals near $\omega=m_p+m_\pi$ contain more events than expected. This discrepancy will be discussed further, when we deal with the $p\pi^-$ system. If these lowest two mass intervals are disregarded, the χ^2 of the fit is 43 for 41 degrees of freedom, giving a probability of 39%. The best values for the intrinsic mass and width of the N^{*++} from this fit are

$$\omega_0=(1.230\pm0.007)\text{GeV},$$
$$\Gamma_0=(0.155\pm0.020)\text{GeV},$$

while the relative abundances of the resonance and phase-space terms are (49 ± 3) and $(51\pm3)\%$, respectively. Since there are two $p\pi^+$ combinations per event, the fit we obtain is consistent with the statement that an N^{*++} is produced in virtually every event with this four-body final state.

Those events (1427 in all) with a $p\pi^+$ mass lying in the range 1.160 to 1.285 GeV were taken as representing a reasonably pure sample in which N^{*++} formation occurs. The amount of nonresonant background in this sample was estimated to be $(17\pm3)\%$. In the same sample it was found that for 1142 of the events only one $p\pi^+$ combination lay within the chosen mass range, so that for the $p\pi^-$ system the choice of the other proton with the π^- was clear. In the remaining 285 events, both $p\pi^+$ combinations lay within the chosen range, but, in each case, the ambiguity could be resolved by demanding that one $p\pi^-$ combination be an $N^{*0}(1236)$. The mass distribution of the 1427 $p\pi^-$ events chosen in this way is shown in Fig. 6 and the presence of the three N^{*0} isobars is clear. As was the case with the $p\pi^+$ spectrum a fit has been made to the data in Fig. 6 using the sum of three resonant cross sections and phase space; in

other words the data were fitted to the equation

$$\frac{dN(\omega)}{d\omega}=[a_0+\sum_{i=1}^{3} a_i R_i(\omega_i,\Gamma_i)]\phi(\omega), \quad (4)$$

in which the multiplicative constants a_i represent the relative production rates of phase space $[\phi(\omega)]$ and resonance $[R_i(\omega_i,\Gamma_i)]$ terms, and R_i is given by (1) using the appropriate value of l in (2). The results of the minimum χ^2 fit shown in Fig. 6 are that the mass, width, and relative abundance of each N^* are

$$\omega_1=(1.240\pm0.006)\text{GeV},$$
$$\Gamma_1=(0.157\pm0.025)\text{GeV},$$
$$a_1=(48\pm5)\%,$$
$$\omega_2=(1.480\pm0.010)\text{GeV},$$
$$\Gamma_2=(0.090\pm0.015)\text{GeV},$$
$$a_2=(8\pm2)\%,$$
$$\omega_3=(1.670\pm0.010)\text{GeV},$$
$$\Gamma_3=(0.080\pm0.020)\text{GeV},$$
$$a_3=(6\pm2)\%.$$

Phase space $(a_0)=(38\pm5)\%$. No interference terms between the resonances or with the nonresonant background have been included in this fit.

As with the fit to the data of Fig. 2, the events near $\omega=m_p+m_\pi$ are poorly represented by this minimum χ^2 fit and the over-all probability is less than 1%. However, if the lowest three mass intervals are disregarded, the probability of fit with the above parameters rises to 81%. To further investigate this effect a "pole-model" calculation of the expected $p\pi^-$ spectrum was made by assuming that a "stable" $N^{*++}(1236)$ isobar is produced at the lower vertex ($b\,e\,d$) of Fig. 4, while the real process ($\pi^-+p\rightarrow\pi^-+p$) occurs at the upper vertex ($a\,e\,c$). Following Chew and Low[8] and Ferrari,[9] we find[1]

$$d\sigma=\frac{G^{*2}}{m_\pi^2}\frac{2}{3}\frac{b_d^2[t-(m_b-m_d)^2]}{8q^2W^2}\frac{1}{8\pi^2}\frac{1}{(m_\pi^2-t)^2}\times\sigma(\omega)K(\omega)dtd\omega^2, \quad (5)$$

where

$$b_d^2=(1/4m_d^2)[t-(m_b-m_d)^2][t-(m_b+m_d)^2],$$
$$K(\omega)=[\tfrac{1}{4}\omega^4+\tfrac{1}{4}(m_a^2-m_\pi^2)^2-\tfrac{1}{2}\omega^2(m_a^2+m_\pi^2)]^{1/2},$$

G^* is the $NN^*\pi$ coupling constant (obtained from the known width Γ of the N^*), ω is the center-of-mass energy of the π^-p system, q and W and the initial center-of-mass momentum and energy, and t the square of the four-momentum transfer.

[8] G. F. Chew and F. E. Low, Phys. Rev. **101**, 1570 (1956).
[9] E. Ferrari, Nuovo Cimento **30**, 240 (1963).

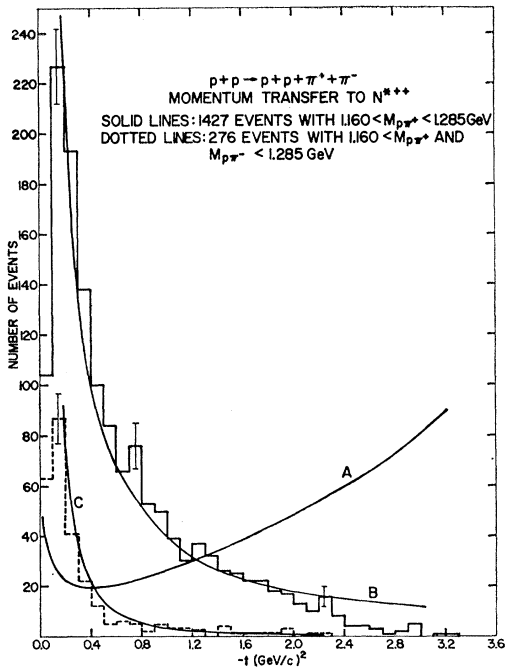

FIG. 7. Momentum transfer to the $N^{*++}(1236)$ of reaction (i). Curve A is the unmodified one-pion-exchange result normalized to the observed cross section. Curves B and C represent the inclusion of a form factor of the type $(\alpha^2-m_\pi^2)/(\alpha^2-t)$.

This equation was integrated over t for each value of ω; in each case the appropriate value of $\sigma(\omega)$ for the π^-p cross section was obtained by interpolation from a table of measured cross sections. The resultant distribution gives the correct shape for the $N^*(1236)$ region from the phase-space threshold up to about 1.3 GeV, where the momentum transfer to the isobar is small. However, the departure from the data becomes very pronounced in the region of the $N^*(1500)$ and $N^*(1688)$, where the allowed momentum transfers are larger resulting in the calculated cross section being larger than the observed one by a factor of 4.3. In an effort to suppress these effects at large values of ω, we include a form factor of the type $F(t)=(\alpha^2-m_\pi^2)/(\alpha^2-t)$ in Eq. (5) and find that with the parameter $\alpha=0.015$ the situation is much improved and the fit produced (including absolute normalization to the experimental cross section) is shown as the broken curve of Fig. 6. It is interesting to note that at low values of the π^-p mass where the phenomenological fit is poor the pole approximation fit gives very good agreement, supporting the assumption that real π^-p scattering takes place at one or both vertices (i.e., part N^{*0} formation and part S-wave scattering). We shall see further evidence for this possibility in the N^*-decay angular distributions presented below.

Additional information on the production mechanism in the single-particle-exchange model can be obtained by examining the momentum-transfer distribution. A plot of the momentum transfer to the N^{*++} isobar

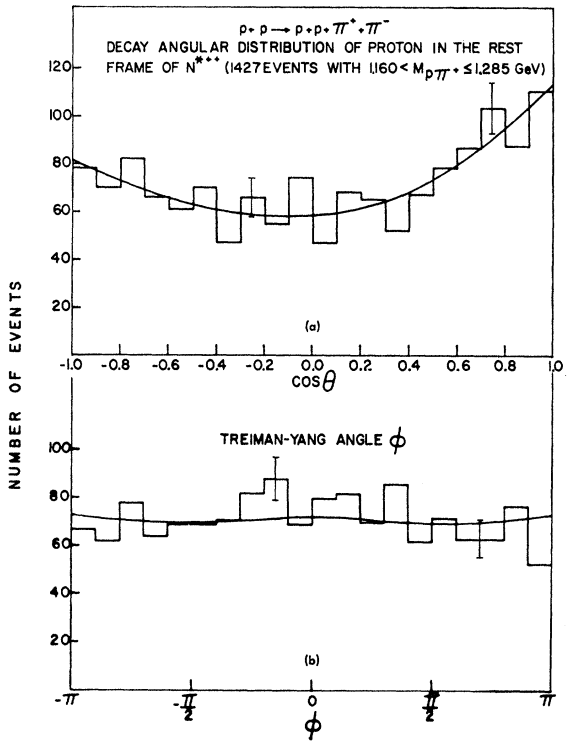

FIG. 8. Jackson parameters of the $N^{*++}(1236)$ system of reaction (i).

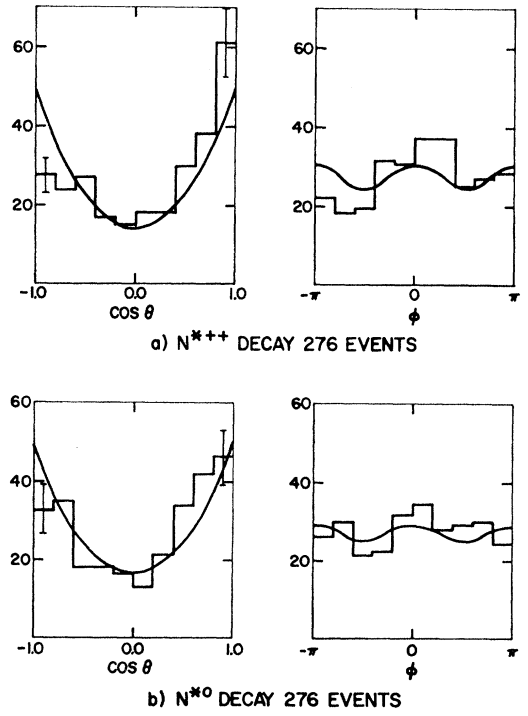

FIG. 9. Jackson parameters of the N^{*++} and N^{*0} systems for double $N^*(1236)$ formation in reaction (i).

(which is taken as being that $p\pi^+$ combination with $1.160<m_{p\pi^+}\leq 1.285$ GeV, any ambiguities being resolved as above) is shown in Fig. 7. The pronounced peaking at small values of momentum transfer is characteristic of a peripheral interaction with the exchange of a light particle. The solid-line histogram of Fig. 7 represents the momentum-transfer distribution to all 1427 N^{*++} isobars while the dotted-line histogram is for 276 events selected as being double $N^*(1236)$ production, namely $p+p\rightarrow N^{*++}+N^{*0}(1236)$. For

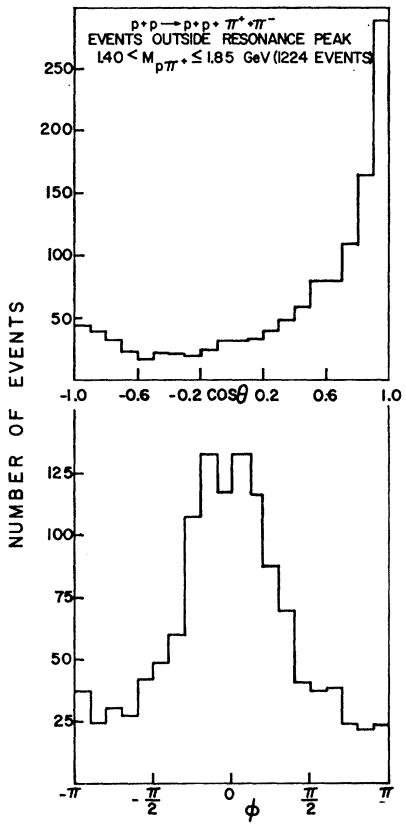

FIG. 10. Jackson parameters of those $p\pi^+$ combinations outside the $N^{*++}(1236)$ peak in reaction (i).

double isobar production the expected momentum-transfer distribution is calculated to be[1]

$$\frac{d\sigma}{dt}=\frac{0.3894}{64\pi W^2q^2}\left\{\frac{G^{*2}}{m_\pi^2}\frac{2}{3}[(m_a+m_c)^2-t]b_d^2\right\}^2\frac{|F(t)|^2}{(m_\pi^2-t)^2}, \quad (6)$$

where all the terms have been defined above and we assume the isobars to be stable particles. Using this equation with $F(t)=1$ we have the unmodified one-pion-exchange result which is shown normalized to 1427 events as curve A of Fig. 7. This curve at first falls as $|t|$ increases owing to the propagator term in Eq. (6). However, this is soon offset by the high powers of t which occur in the numerator (an extra power of t^2

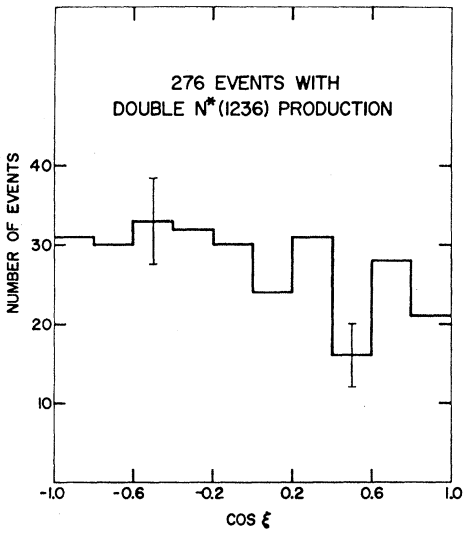

FIG. 11. Correlation between the two final-state protons from double $N^*(1236)$ events in reaction (i).

enters each time the spin of one of the outgoing particles, c or d, is raised by 1). Curve B has the form factor $F(t)=(\alpha^2-m_\pi^2)/(\alpha^2-t)$ included and with $\alpha^2=0.2$; this clearly represents a better fit to the data than curve A. In the case of the 276 events selected for double $N^*(1236)$ production the best fit of the data using the above form factor in Eq. (6) is given for $\alpha^2=0.01$.

The decay angular distributions of a resonance may be used to evaluate certain elements of the density matrix of the resonance and so obtain further information on the production mechanism involved. We first consider the 1427 events with an N^{*++} resonance in the $p\pi^+$ spectrum. To define our coordinate system we have to decide whether the N^{*++} is produced at the vertex with the beam proton or at the vertex with the target proton (Fig. 4). To do this we choose the "incoming" particle to be that proton which would give the smaller momentum transfer to the N^{*++}. From Fig. 5 we estimate that no more than 7% of the events will have the incident proton incorrectly chosen by this technique. A Lorentz transformation is now made to the rest frame of the resonance and the decay distributions in $\cos\theta$ and ϕ (the "Jackson parameters"; ϕ is also the Yang-Treiman angle) of the proton from the N^{*++} decay found relative to the production plane in this system. The results are shown in Fig. 8. The expected decay angular distributions of a spin-$\frac{3}{2}$ resonance are given in terms of the density matrix elements $\rho_{i,j}$ by[10]

$$\frac{dW(\cos\theta)}{d(\cos\theta)}=\tfrac{3}{4}\pi\{\tfrac{1}{3}(1+4\rho_{3/2,3/2})+(1-4\rho_{3/2,3/2})\cos^2\theta\} \quad (7)$$

and

$$\frac{dW(\phi)}{d\phi}=\tfrac{1}{2}\{1-(\sqrt{\tfrac{4}{3}})\,\mathrm{Re}\rho_{3/2,-1/2}+(\sqrt{8/3})\,\mathrm{Re}\rho_{3/2,-1,2}\sin^2\phi\}, \quad (8)$$

with the unitarity requirement on the density matrix that $\rho_{3/2,3/2}+\rho_{1/2,1/2}=0.5$. The predictions of the unmodified one-pion-exchange model are that $\rho_{3/2,3/2}=\mathrm{Re}\rho_{3/2,-1/2}=0$. Applying these results to the 1427 N^{*++} events shown in Fig. 8, a minimum χ^2 fit was performed in each case. With a 20% probability the data of

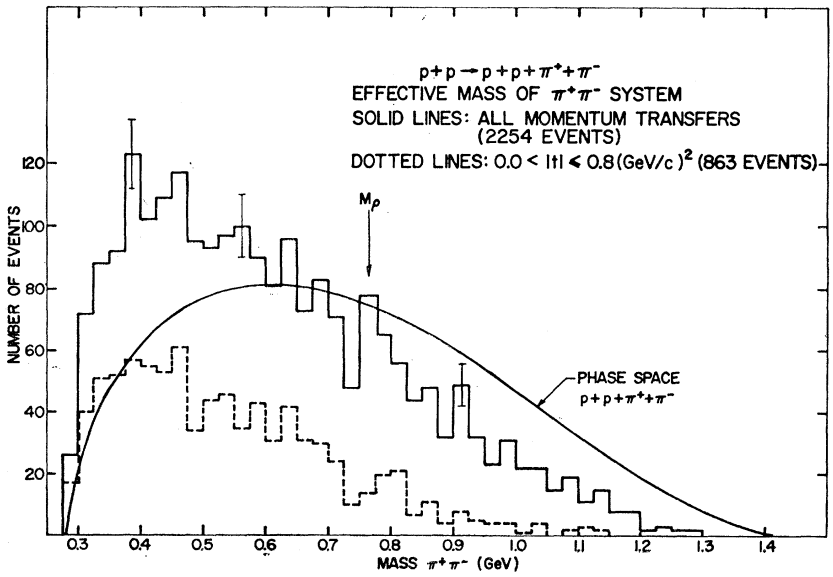

FIG. 12. Effective mass of the $\pi^+\pi^-$ system for reaction (i).

[10] J. D. Jackson, Rev. Mod. Phys. 37, 484 (1965).

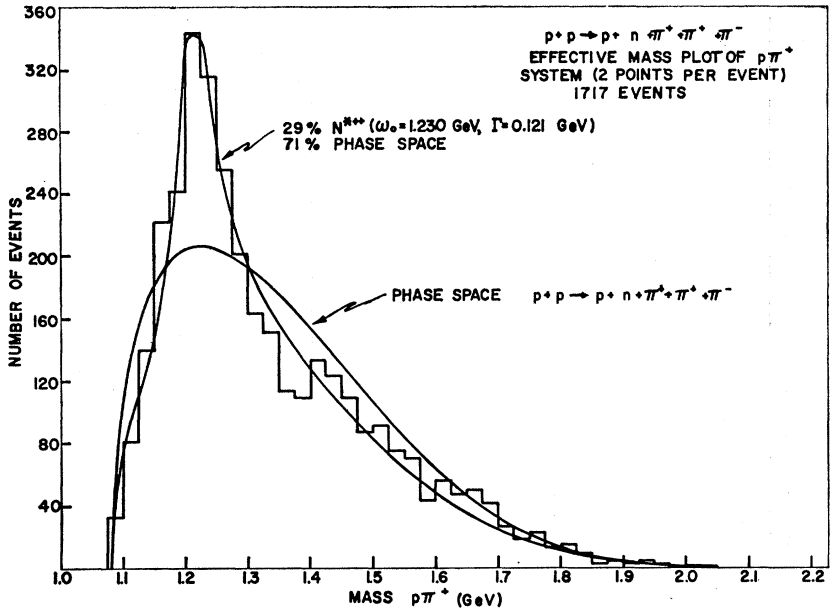

FIG. 14. Effective mass of the $p\pi^+$ system for reaction (ii).

Fig. 8(a) was fitted by the equation

$$dW(\cos\theta)/d(\cos\theta)=58.50(1.00+0.13\cos\theta+0.67\cos^2\theta+0.15\cos^3\theta). \quad (9)$$

A comparison with Eq. (7) shows that the coefficients of the odd powers in $\cos\theta$ should be zero; in fact they are only about one-quarter of the magnitude of that of the $\cos^2\theta$ term and to the extent that they can be neglected (we may regard them as due to interference with the nonresonant background) we obtain for the density matrix element $\rho_{3/2,3/2}$ the value

$$\rho_{3/2,3/2}=0.15\pm0.02. \quad (10)$$

Similarly for Fig. 8(b) we find the best solution (20% probability) to be

$$dW(\phi)/d\phi=72.00(1.00-0.02\sin^2\phi). \quad (11)$$

In this case the distribution is sufficiently isotropic that terms in odd powers of $\sin\phi$ are negligible. A comparison of (11) with Eq. (8) gives the result

$$\mathrm{Re}\rho_{3/2,-1/2}=0.00\pm0.01. \quad (12)$$

From these figures we see that $\rho_{3/2,3/2}$ does not agree with the value predicted for one-pion exchange, although $\mathrm{Re}\rho_{3/2,-1/2}$ is consistent with such an exchange mechanism. It is instructive to see if these density matrix elements have any marked dependence on the momentum transfer. To do this, the sample of the 1427 N^{*++} events, which include all momentum transfers, has been divided into groups with increasing momentum transfers and the decay distributions determined as before. The results are shown in Table II; the ranges of momentum transfer were chosen so that approximately equal numbers of events would fall into each category. It will be noticed that at small momentum transfers the density matrix elements certainly approach the values predicted by the single-pion-exchange model but that the deviation from these predictions becomes larger as $|t|$ increases and this could be attributed to absorption effects.[10] It is found that absorption causes larger changes in $\rho_{3/2,3/2}$ than in $\mathrm{Re}\rho_{3/2,-1/2}$, so that even as the distribution $W(\cos\theta)$ is shifted rapidly away from the $1+3\cos^2\theta$ form expected for pseudoscalar exchange, the distribution in ϕ can remain nearly isotropic.[11] In fact, the expected effect of the absorptive process is to shift $\rho_{3/2,3/2}$ approximately linearly from ~0.08 at $t=-0.1(\mathrm{GeV}/c)^2$ to ~0.20 at $t=-1.0(\mathrm{GeV}/c)^2$, while in the same interval $\mathrm{Re}\rho_{3/2,-1/2}$ changes from 0.0 to 0.06. This is very close

TABLE II. Density matrix elements of the N^{*++} produced in the reaction $p+p\to p+p+\pi^++\pi^-$.

Interval momentum transfer $\lvert t\rvert$ (GeV/c)^2	Number of events in interval	$\rho_{3/2,3/2}$	$\rho_{1/2,1/2}$	Re $\rho_{3/2,-1/2}$
0.0–0.2	331	0.06±0.04	0.44±0.04	−0.03±0.02
0.2–0.4	321	0.13±0.03	0.37±0.03	−0.02±0.02
0.4–0.8	326	0.23±0.03	0.27±0.03	−0.01±0.02
0.8–1.6	292	0.20±0.03	0.30±0.03	0.05±0.02
1.6–3.4	147	0.27±0.05	0.23±0.05	0.06±0.03
0.0–3.4	1427	0.15±0.02	0.35±0.02	0.004±0.01
One-pion-exchange model	···	0.0	0.5	0.0

[11] G. Alexander, B. Haber, A. Shapira, G. Yekutieli, and E. Gotsman, Phys. Rev. 144, 1122 (1966).

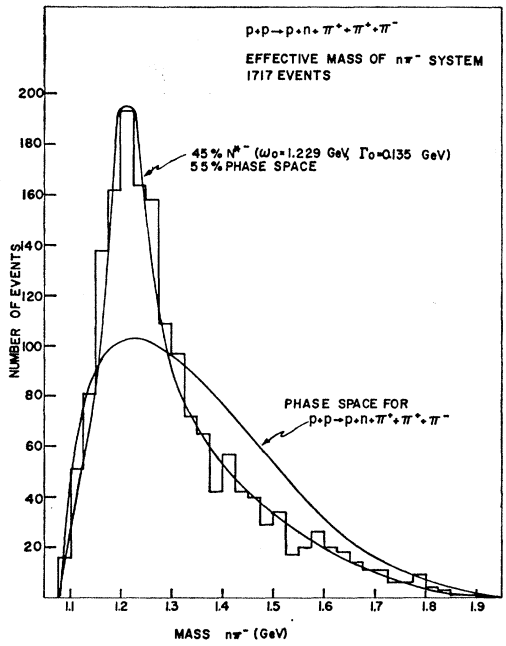

FIG. 13. Effective mass of the $n\pi^-$ system for reaction (ii).

to the shifts observed in our data, so it is reasonable to conclude that absorptive effects enter this reaction and become increasingly important as $|t|$ increases.

We have also studied those events in which double $N^*(1236)$ formation occurs. Of the 1427 N^{*++} events discussed so far 276 events were selected in which there was an unambiguous combination $p\pi^+$ and $p\pi^-$ both of which has a mass in the range 1.160 to 1.285 GeV.

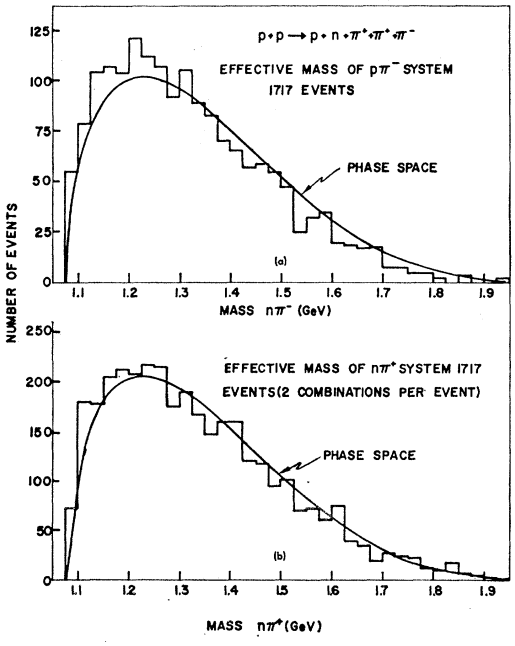

FIG. 15. Effective mass of the $p\pi^-$ and $n\pi^+$ systems of reaction (ii).

The decay angular distributions of these events are shown in Fig. 9. Both the N^{*++} and N^{*0} decay distributions are seen to be characteristic of pseudoscalar exchange and the density matrix elements for the two isobars using this sample have been found to be

$$N^{*++}: \quad \rho_{3/2,3/2}=0.04\pm0.04, \quad \mathrm{Re}\rho_{3/2,-1/2}=0.04\pm0.02, \tag{13}$$

$$N^{*0}: \quad \rho_{3/2,3/2}=0.05\pm0.04, \quad \mathrm{Re}\rho_{3/2,-1/2}=0.03\pm0.02. \tag{14}$$

Here again we observe the presence of odd powers of $\cos\theta$ with a magnitude of about one-quarter that of the term in $\cos^2\theta$. The forward-backward asymmetry

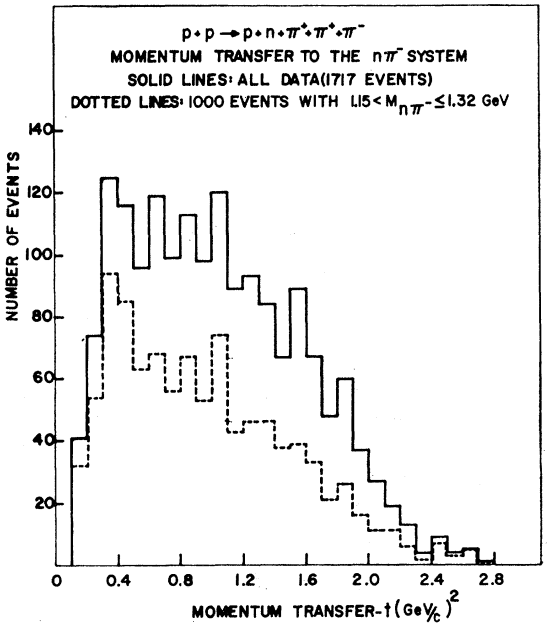

FIG. 16. Momentum-transfer distribution to the $n\pi^-$ system of reaction (ii).

seen in Figs. 8 and 9 which gives rise to these odd powers of $\cos\theta$ is in itself interesting since the same situation has been observed many times in counter experiments involving real $\pi^\pm p$ scattering.[12] In such experiments which investigate the region of the $N^*_{3/2,3/2}$ resonance (lab K.E. of pions$\simeq$200 MeV) it is found that the differential cross section as a function of the center-of-mass scattering angle θ gives the expected $1+3\cos^2\theta$ form. However, as the kinetic energy of the pion is raised (corresponding to raising the πp effective mass), odd powers of $\cos\theta$ quickly enter and the distribution becomes very asymmetrical. This is precisely the situa-

[12] J. Ashkin, J. P. Blaser, F. Feiner, and M. O. Stern, Phys. Rev. **101**, 1149 (1956); J. A. Helland, T. J. Devlin, D. E. Haage, M. J. Longo, B. J. Moyer, and C. D. Wood, *ibid.* **134**, B1062 (1964); E. Gellert, G. A. Smith, S. Wojciki, E. Colton, P. E. Schlein, and H. K. Ticho, Phys. Rev. Letters **17**, 884 (1966).

tion we observe in the present data; for example, if we select from the $p\pi^+$ spectrum of Fig. 2 those events with $1.40<m_{p\pi^+}\leq 1.85$ GeV (i.e., no combination in the resonance region) and plot their decay distributions as though they were N^* events, we obtain the results shown in Fig. 10. The distribution in $\cos\theta$ corresponds closely to that seen in counter experiments for the same $p\pi$ effective mass. The distribution in ϕ shown in Fig. 10 is far from isotropic and appears to be completely incompatible with a single-pion-exchange process. We cannot satisfactorily account for this high degree of alignment of the production and decay planes at the present time, though it is interesting to note that a similar effect has been reported[11] in the reaction $p+p\rightarrow n+N^{*++}(1238)$ at 5.5 GeV/c.

One final remark may be made about this four-body final state in which 2 $N^*(1236)$ isobars are produced. It

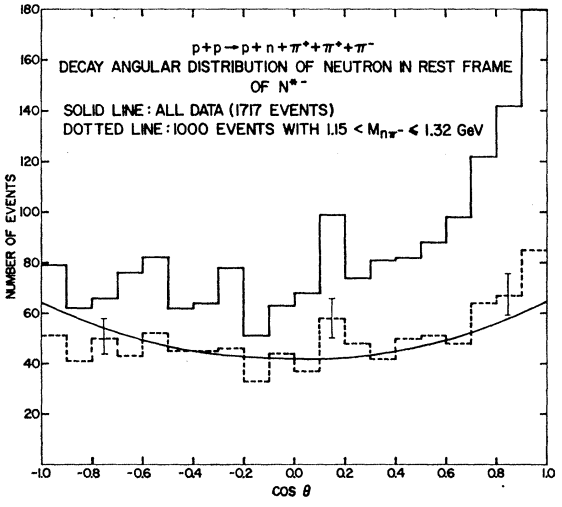

FIG. 17. Decay angular distribution, $\cos\theta$, of the neutron in the rest frame of the N^{*-} for reaction (ii).

is interesting to look for the presence of ρ-meson exchange in these events. If the ρ meson is coupled to the $N^*(1236)$ isobar in the manner predicted by the Stodolsky-Sakurai model,[13] then the presence of such an exchange mechanism would manifest itself by a correlation between the directions of the nucleons from the isobar decays.[1] We define

$$\cos\xi=\frac{(\mathbf{P}_\alpha)_d\cdot(\mathbf{P}_{\alpha'})_c}{|(\mathbf{P}_\alpha)_d||(\mathbf{P}_{\alpha'})_c|}, \tag{15}$$

where $(\mathbf{P}_\alpha)_d$ and $(\mathbf{P}_{\alpha'})_c$ represent the 3-momenta of the protons from the $(N^*)_d$ (say the N^{*++}) and the $(N^*)_c$ (say the N^{*0}) in their respective center-of-mass systems. Then the value of $\cos\xi$ is calculated for each of the 276 double $N^*(1236)$ events and the results plotted in

[13] L. Stodolsky and J. J. Sakurai, Phys. Rev. Letters **11**, 90 (1963); L. Stodolsky, Phys. Rev. **134**, B1099 (1964).

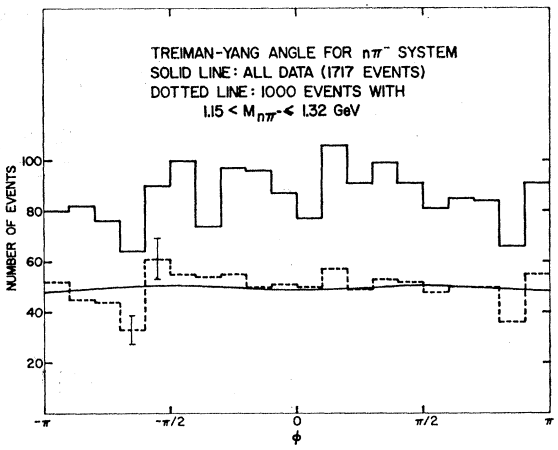

FIG. 18. Treiman-Yang angle for the neutron from the N^{*-} for reaction (ii).

Fig. 11. The data is consistent with an isotropic distribution in $\cos\xi$ (the probability is 35%), indicating that there is no evidence for ρ exchange in this sample. We also see from the $\pi\pi$ mass distribution for all events with this four-body final state that there is no evidence for ρ-meson production (Fig. 12).

B. The Reaction $p+p\rightarrow p+n+\pi^++\pi^++\pi^-$

The formation of nucleon isobars in this reaction occurs almost entirely through $I=\frac{3}{2}$ channels. The $n\pi^-$ system is dominated by the $N^{*-}(1236)$ as is seen in Fig. 13 and a fit using Eq. (3) gives the mass and width

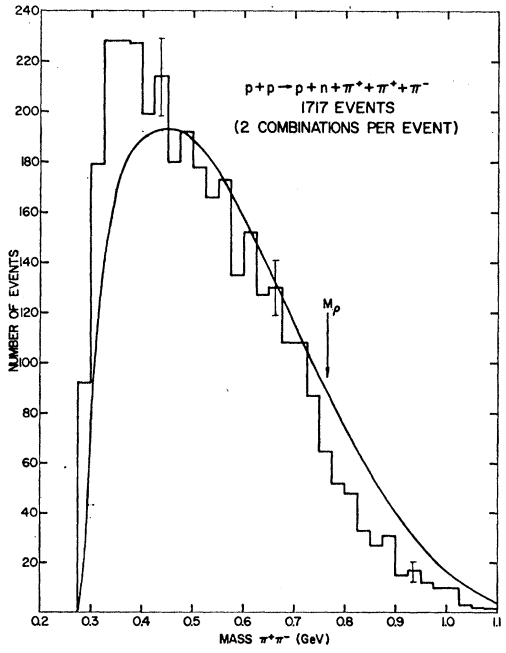

FIG. 19. Effective mass of the $\pi^+\pi^-$ system in reaction (ii).

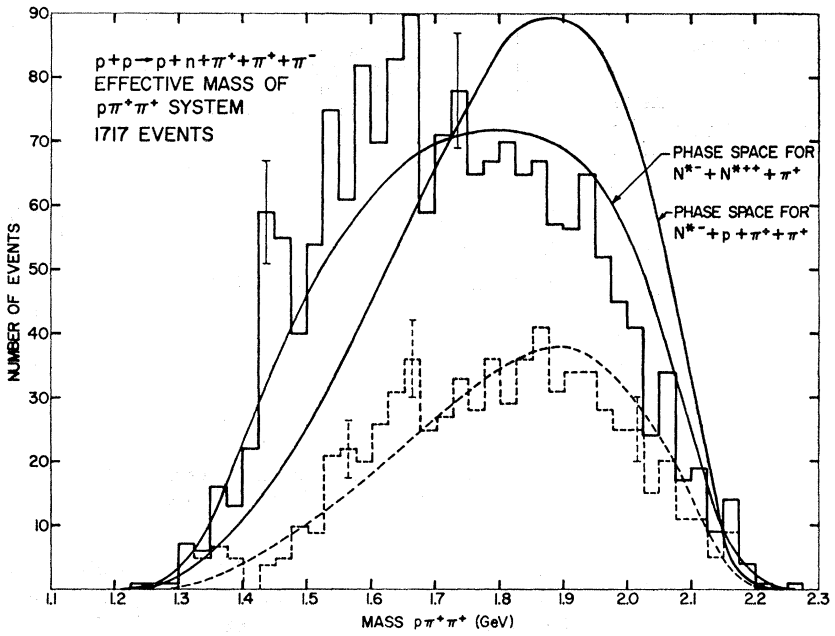

FIG. 20. Effective mass of the $p\pi^+\pi^+$ system in reaction (ii). The solid histogram is for all 1717 events while the broken histogram represents 719 events with no N^{*++} in the range $1.175 \leq m_{p\pi^+} < 1.275$ GeV.

of this isobar (with 15% probability) as

$$N^{*-}: \quad \omega_0 = 1.229 \pm 0.008 \text{ GeV},$$
$$\Gamma_0 = 0.135 \pm 0.020 \text{ GeV},$$

with the percentage of phase space as $(55 \pm 5)\%$. Similarly, the $p\pi^+$ system, which is shown in Fig. 14, is found to contain $(71 \pm 7)\%$ phase space while the mass and width of the N^{*++} are given (with 5% probability) by

$$N^{*++}: \quad \omega_0 = 1.230 \pm 0.009 \text{ GeV},$$
$$\Gamma_0 = 0.121 \pm 0.028 \text{ GeV},$$

In this case there are two $p\pi^+$ combinations plotted per event because of the occurrence of two positive pions in the final state. The π-nucleon mass distributions for the $I = \frac{1}{2}$ systems are shown in Fig. 15.

Because of the presence of the extra pion in the final state, it becomes very hard to make any strong arguments about the mechanism through which the resonances are produced since we do not know to which vertex this pion is attached. One possibility is for the $n\pi^-$ system to occur alone at one vertex and from charge conservation this would require the exchange in the simplest of cases of two singly charged particles. If this were the situation, we would expect a very broad momentum-transfer distribution to the $n\pi^-$ system which is, in fact, seen to be the situation in Fig. 16. Another possibility is that the $\rho\pi^+$ system occurs at one vertex and that one pion exchange would be dominant. In this case we would expect the momentum-transfer distribution to the $p\pi^+$ system to be characteristically peaked at small $|t|$; this is not observed—the momentum-transfer distribution is very similar to that shown for the $n\pi^-$ in Fig. 16. There is also the possibility that there could be an arbitrary admixture of these two processes or that some much more complex exchange mechanism dominates the reaction.

If we plot the decay angular distributions of the $n\pi^-$ system, we obtain the results shown in Figs. 17 and 18. The solid-line histograms refer to all 1717 $n\pi^-$ events (the combination is unambiguous), while the dotted-line histograms represent only those 1000 events in the N^{*-} region ($1.15 < m_{n\pi^-} \leq 1.32$ GeV). It is very interesting to note that the Yang-Treiman angle (Fig. 18) is consistent with isotropy even when all 1717 events are included (contrast this with Fig. 10). However, the distribution in $\cos\theta$ is seen to become more asymmetrical as events outside the N^{*-} region are included (Fig. 17). The result of fitting the decay angular distributions of those events in the N^{*-} region gives the following two density matrix values:

$$\rho_{3/2,3/2} = 0.17 \pm 0.02 \quad (5\% \text{ probability}),$$
and (16)
$$\mathrm{Re}\rho_{3/2,-1/2} = 0.01 \pm 0.01 \quad (60\% \text{ probability}).$$

No significant results could be obtained on the $p\pi^+$ system because of the large amount of nonresonant background.

The $\pi^+\pi^-$ mass distribution is shown in Fig. 19 (two combinations per event) and again there is no evidence for ρ-meson production.

Evidence has been reported[14] for the possible existence of an $I = \frac{5}{2}$ nucleon isobar in the $p\pi^+\pi^+$ system

[14] G. Goldhaber, S. Goldhaber, T. O'Halloran, and B. C. Shen, in *12th Annual Proceedings of the International Conference on High Energy Physics, Dubna, 1964* (Atomizdat, Moscow, 1965); G. Goldhaber, in *Proceedings of the Second Coral Gables Conference on Symmetry Principles at High Energies, Miami, 1965* (W. H. Freeman and Company, San Francisco, California, 1965); G. Alexander, P. Benary, B. Reuter, A. Shapira, E. Simopoulou, and G. Yekutieli, Phys. Rev. Letters 15, 207 (1965).

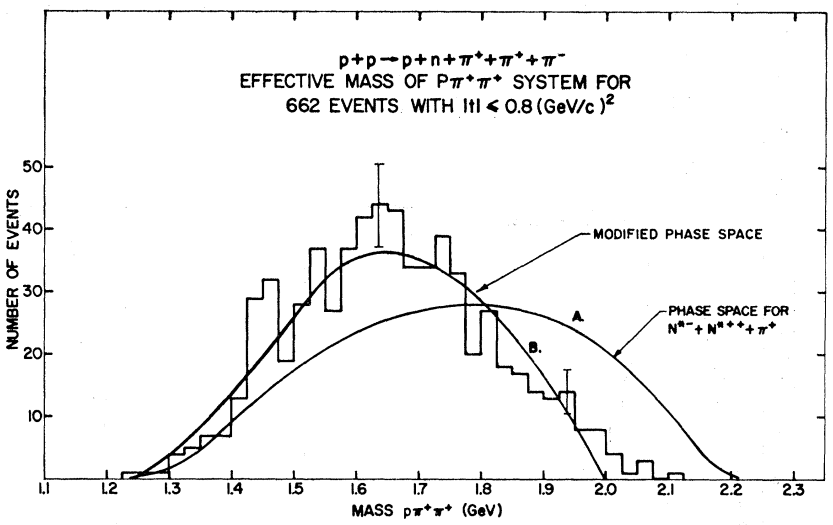

FIG. 21. Effective mass of the $p\pi^+\pi^+$ system for those events with $|t|\leq 0.8$ $(\mathrm{GeV}/c)^2$ in reaction (ii).

with a mass of 1.58 GeV and a width of 0.2 GeV. This possibility is interesting because it would agree with the supposition that the $n\pi^-$ system occurs alone at one vertex and hence the broad momentum-transfer distribution to this system could be qualitatively understood. The $p\pi^+\pi^+$ mass distribution of our data is shown in Fig. 20 and if the four-body phase space for the final-state $N^{*-}p\pi^+\pi^+$ is used, a departure of the data from the theoretical curve exists in the region below 1.7 GeV. If, however, the phase space for the three-body final state $N^{*-}+N^{*++}+\pi^+$ is used (which is more appropriate since both N^{*++} and N^{*-} occur) the deviation from the expected distribution is much less pronounced—no data point is more than two standard deviations away from this phase-space curve. If we remove events with a possible N^{*++}, the 719 events remaining form the broken histogram shown in Fig. 20. Again we see that the four-body phase space (the broken curve on this histogram) fits the data poorly, but that if any enhancement exists it is at 1.65 GeV, not 1.58 GeV.

When the restriction is imposed that the momentum transfer to the $p\pi^+\pi^+$ system be less than 0.8 $(\mathrm{GeV}/c)^2$, the distribution shown in Fig. 21 is obtained. The $N^{*++}N^{*-}\pi^+$ phase space shown as curve A in Fig. 21 can no longer be said to represent the data well but the observed depletion of events in the region with $m_{p\pi\pi}>1.8$ GeV can be due to the fact that restrictions have been made on the momentum transfer. The phase-space curve A must now be modified by some function $f(t)$ which, in general, will be a dynamical factor dependent upon the production model (which is unknown in the present case). For example, curve B was obtained by defining

$$f(t)=0.8-|t|_{\min}(\omega), \qquad (17)$$

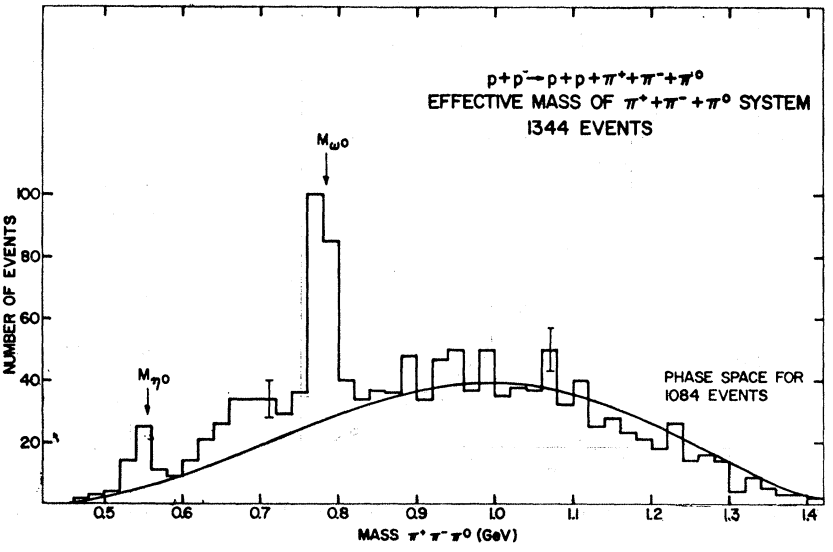

FIG. 22. Effective mass of the $\pi^+\pi^-\pi^0$ system in reaction (iii).

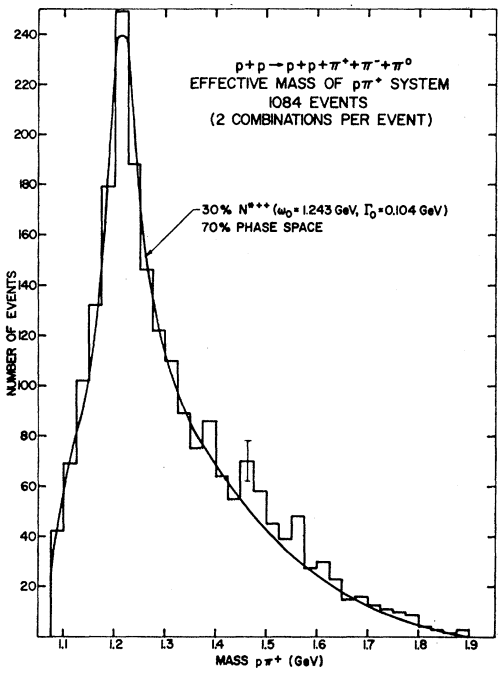

FIG. 23. Effective mass of the $p\pi^+$ system in reaction (iii).

where $|t|_{\min}(\omega)$ is the minimum possible value of the momentum transfer when the $p\pi^+\pi^+$ system has a mass ω and the $n\pi^-$ occurs as an $N^*(2316)$. The resultant curve is seen to adequately represent the data for this low-momentum-transfer region and we conclude that there is no significant evidence in this reaction channel for the existence of an $I=\frac{5}{2}$ isobar. A possible way of verifying the absence or presence of such a resonance would be to repeat the experiment at higher values of

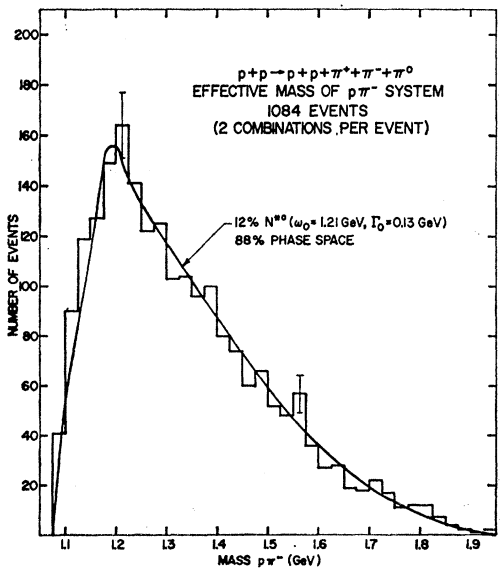

FIG. 24. Effective mass of the $p\pi^-$ system in reaction (iii).

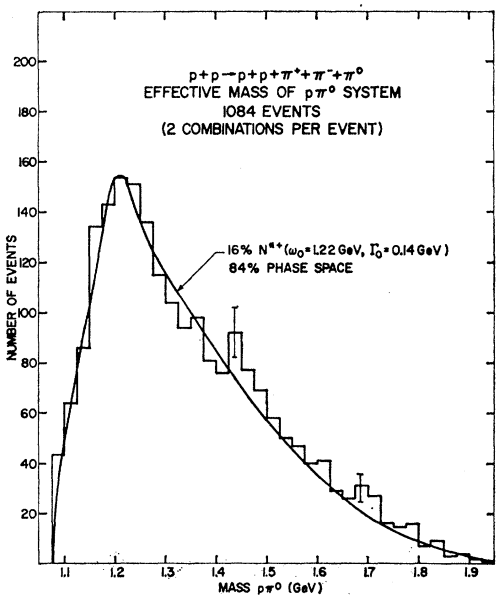

FIG. 25. Effective mass of the $p\pi^0$ system in reaction (iii).

the center-of-mass energy where $|t|_{\min}(\omega)$ would be a much less sensitive function of ω for values of the combined mass near 1.8 GeV.

C. The Reaction $p+p\rightarrow p+p+\pi^++\pi^-+\pi^0$

Because this final state contains the π^+, π^-, and π^0 mesons, the possibility of ω- and η-meson production exists. The $\pi^+\pi^-\pi^0$ spectrum for 1344 events identified

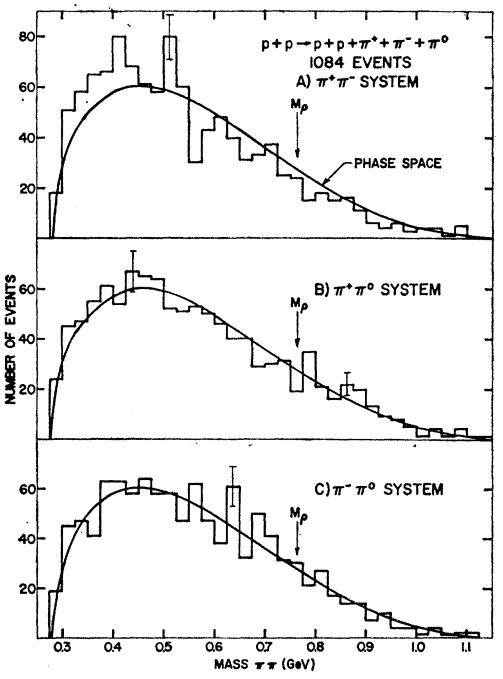

FIG. 26. Effective mass of the two-pion systems in reaction (iii).

with this final state is shown in Fig. 22. The ω^0 and η^0 production cross sections are (0.17 ± 0.02) mb and (0.12 ± 0.04) mb, respectively, when the decay branching ratios are taken into account.

Those events in which the three pions have an ω or η mass were removed from the sample and the mass distributions of the $p\pi^+$, $p\pi^-$, and $p\pi^0$ systems for the remaining 1084 events are shown in Figs. 23, 24, and 25, respectively. The presence of $N^{*++}(1236)$ is clear and some $N^{*0}(1236)$ and $N^{*+}(1236)$ formation occurs, but in all cases the large amounts of nonresonant background present preclude any meaningful determination of the density matrix elements.

In Fig. 26 we show the $\pi\pi$ mass spectra and, as in the previous two reactions, there is no evidence for ρ-meson production.

ACKNOWLEDGMENTS

We would like to thank the crew of the Brookhaven 80-in. bubble chamber and the staff of the alternating gradient synchrotron for their excellent cooperation. We also want to thank E. Hart, R. Rau, and V. Barnes for their assistance in the determination of the bubble-chamber constants, and D. Rahm, I. Skillicorn, and M. Webster who worked on the beam. It is a pleasure to acknowledge the excellent work of our scanning and measuring staff and the help given to us at every stage of the analysis by E. Bierman.

PHYSICAL REVIEW VOLUME 161, NUMBER 5 25 SEPTEMBER 1967

Complex Angular Momentum and Infinite Helicity Sums*

IAN T. DRUMMOND AND G. A. WINBOW
Department of Applied Mathematics and Theoretical Physics, University of Cambridge, Cambridge, England
(Received 30 March 1967)

Previous discussions of the continuation to complex angular momentum of three-particle unitarity integrals for simple diagrams are reformulated in terms of infinite helicity sums. This is achieved by a redefinition of the partial-wave projection of the production amplitudes. It is found that the helicity sums can be made to converge by suitable choice of complex contours for the phase-space integral. It is shown that this leads to the same results as found previously without the introduction of helicity sums.

INTRODUCTION

SOME progress has been made recently[1–5] in understanding the properties of three-particle unitarity integrals continued to complex values of the total angular momentum J. The particular problem considered was the contribution $\Delta_{3\pi}T_{AB}$ of a three-particle state (π_1,π_2,π_3) to the energy discontinuity of a two-particle elastic-scattering amplitude T_{AB}. (We use the notation of Ref. 1.) Asimov *et al.*[3,4] have suggested some heuristic methods for dealing with this situation in general but exact results have been obtained only for the amplitudes of the type associated with Figs. 1 and 2 and simple generalizations of them.[2,5]

A reason why these amplitudes have proved tractable is that in the intermediate state at least one pair of particles exists only in a relative S wave. If partial-wave production amplitudes are defined in a way which emphasizes this, then it is possible to avoid the problem of infinite helicity sums when continuing to arbitrary values of J.

However, at least one pair of the three intermediate-state particles can exist in any relative angular-momentum state. If a definition of partial waves is used which emphasizes this, then summation over an infinite number of helicities is necessary. In this paper we wish to analyze the diagrams of Figs. 1 and 2 with such a definition of partial waves in order to obtain insights which may help in more general situations where the infinite helicity sums are unavoidable.

1. NOTATION AND DEFINITION OF PARTIAL WAVES

We consider the same reactions as in Ref. 1, where the kinematics are discussed in detail. The amplitudes for the processes

$$A(p_A)+B(p_B)\leftrightarrow A(p_A')+B(p_B'), \quad (1)$$

$$A(p_A)+B(p_B)\leftrightarrow \pi(p_1)+\pi(p_2)+\pi(p_3), \quad (2)$$

* The research reported in this document has been sponsored in part by the Air Force Office of Scientific Research under Grant No. AF EOAR 65-36 through the European Office of Aerospace Research (OAR), U. S. Air Force.

[1] Ian T. Drummond, Phys. Rev. **140**, B1368 (1965).
[2] Ian T. Drummond, Phys. Rev. **153**, 1565 (1967); **155**, 1749 (1967).
[3] Ya. I. Asimov, A. A. Ansel'm, V. N. Gribov, G. S. Danilov, and I. T. Dyatlov, Zh. Eksperim. i Teor. Fiz. **48**, 1776 (1965) [English transl.: Soviet Phys.—JETP **21**, 1189 (1965)].
[4] Ya. I. Asimov, A. A. Ansel'm, V. N. Gribov, G. S. Danilov, and I. T. Dyatlov, Zh.Eksperim. i Teor. Fiz. **49**, 549 (1965) [English transl.: Soviet Phys.—JETP **22**, 383 (1966)].
[5] Ya. I. Asimov, V. N. Gribov, G. S. Danilov, and I. T. Dyatlov, Yadern. Fiz. **1**, 9[illegible] (1965) [English transl.: Soviet J. Nucl. Phys. **1**, 671 (1965)].